Oct 19th, 12:00 AM

Pull-through Failures of Crest-fixed Steel Claddings Initiated by Transverse Splitting

Dhammika Mahaarachchi

Mahen Mahendran

Fifteenth International Specialty Conference on Cold-Formed Steel Structures
St. Louis, Missouri U.S.A., October 19-20, 2000

Pull-through Failures of Crest-fixed Steel Claddings Initiated by Transverse Splitting

By Dhammika Mahaarachchi[1] and Mahen Mahendran[2]

Summary

Crest-fixed steel claddings made of thin, high strength steel often suffer from local pull-through failures at their screw connections during high wind events such as storms and hurricanes. Currently there aren't any adequate design provisions for these cladding systems except for the expensive testing provisions. Since the local pull-through failures in the less ductile steel claddings are initiated by transverse splitting at the fastener hole, analytical studies have not been able to determine the pull-through failure loads. Analytical studies could be used if a reliable splitting criterion is available. Therefore a series of two-span cladding tests was conducted on a range of crest-fixed steel cladding systems under simulated wind uplift loads. The strains in the sheeting around the critical fastener holes were measured until the pull-through failure. This paper presents the details of the experimental investigation and the results including a strain criterion for the local pull-through failure.

1. Introduction

In Australia and its neighbouring countries, trapezoidal and corrugated steel roof claddings made of thin, high strength steel G550 (0.42 mm base metal thickness and minimum yield stress 550 MPa) are used commonly in the building industry. These claddings are always crest-fixed when used as roof cladding as shown in Figure 1. The connection between roof sheeting and battens/purlins is often the weakest link in the structural system when subjected to wind uplift loading. The loss of roofing results in severe damage to the entire building and its contents. This situation is continuing because of the lower priority given to the design of roof and wall cladding systems.

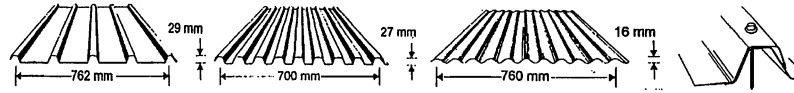

Figure 1. Standard Profiled Steel Cladding Systems used in Australia

Field and laboratory investigations and past researches (Mahendran, 1994, Beck and Stevens, 1979, Xu and Reardon, 1993) have shown that loss of steel roofs has often occurred due to local failures of their screwed connections. The presence of large stress concentration around the fastener hole under wind uplift loading is attributed to the local pull-through or pull-over failures at screwed connections in which the roof sheeting is pulled through or pulled over the fastener heads (see Figure 2a).

1. PhD Scholar 2. Associate Professor of Civil Engineering, and Director
Physical Infrastructure Centre, School of Civil Engineering,
Queensland University of Technology, Brisbane, QLD 4000, Australia

These failures are initiated by a transverse split at the screw hole (Mahendran, 1990a,b, Mahendran and Tang, 1999). For some steel roofing, a local dimpling failure occurs without any transverse splitting and a pull-through failure (see Figure 2b). In this case the disengagement of sheeting does not occur and it is a preferred failure mode. Past research has shown that the stress/strain patterns around the fastener hole are very complicated. However, it is considered that there must be a unique criterion for the transverse split caused pull-through failures. This paper is therefore aimed at determining this criterion, which can be used in the numerical modelling of crest-fixed steel claddings.

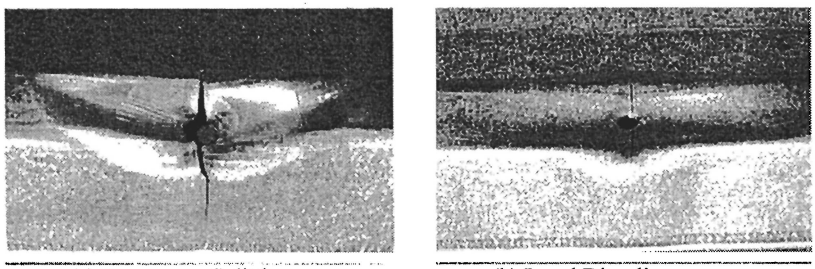

(a) Transverse Splitting (b) Local Dimpling

Figure 2. Local Failures at Screwed Connections

Currently, the Australian cold-formed steel structures standard AS 4600 (SA, 1996) gives the following formula for screwed connections in tension.

$$F_{ov}=1.5\ t\ d_w\ f_u \qquad (1)$$

where t = thickness of steel cladding material

d_w = larger value of the screw head or the washer diameter ≤12.5 mm

f_u = ultimate tensile strength of steel

However, its accuracy for the pull-through strength of crest-fixed claddings is questionable, and thus cladding manufacturers rely on an expensive testing process. Recently, Mahendran and Tang (1999) have developed a design formula for the pull-through strength of crest-fixed steel claddings.

$$F_{ov}= c\ d^{\alpha}\ t^{\beta}\ f_u^{\chi} \qquad (2)$$

where constants c = 0.22,0.23, α = 0.4,0.2, β = 2.2,1.7, χ = 0.4,0.4 for trapezoidal claddings Type A and Type B, respectively

However their research was mainly based on small-scale tests, and has not resolved the issue/ criterion of splitting at the screw holes.

Since the local pull-through failures in the less ductile G550 steel claddings are initiated by transverse splitting at the fastener hole, Tang (1998) found that the finite element analyses could not predict the failure loads as elastic- perfect plastic material behaviour with infinite ductility is assumed without any allowance for splitting. Analytical studies could be used only if a reliable splitting criterion is available. Therefore a series of full-scale tests were conducted on a range of crest-fixed steel cladding systems under simulated wind uplift loads using a large air-box. The strains in the sheeting around the critical fastener hole were measured until the pull-through failure occurred. The strain results were then used to develop a strain criterion. The

failure loads were also used to calibrate the design formula (Equation 2) developed recently from small-scale tests. This paper presents the details of this experimental investigation and the results.

2. Experimental Method

The past analyses of a multi-span roofing assembly have indicated that the critical second support from the eaves or ridge of the roof is adequately represented by the central support of a two-span roofing assembly. Therefore in this experimental investigation, a two-span roofing assembly with simply supported ends was tested under a wind uplift pressure loading (see Figure 3a). In order to accurately simulate a uniform wind uplift pressure and its effects, an air box measuring 1800 mm wide by 4200 mm long by 300 mm deep was used. The test roofing assembly was set-up up side down in the air-box, which was then sealed with 4.5 μm polythene sheets. The uniform wind uplift pressure was simulated by extracting the air from the air box using a vacuum pump. Most of the test roofing assemblies were 800 mm wide (one sheet wide) × 2000 mm long (each span 900-1100 mm). The gaps on both sides of the roofing assembly were filled with polystyrene foam. Bricks were used around the perimeter to keep the polythene sheet intact (see Figure 3b).

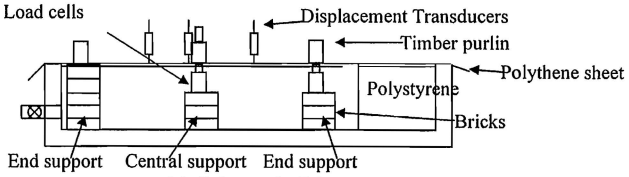

(a) Schematic Diagram

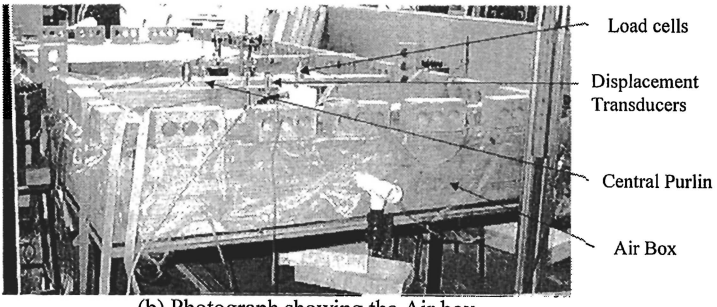

(b) Photograph showing the Air box

Figure 3. Experimental Set-up

The trapezoidal Type A (Figure 1) roofing sheets were fastened at every crest whereas trapezoidal Type B and corrugated roofing sheets were fastened at alternate crests as recommended by the manufacturers. The No.14-10x50 mm Type 17 self-drilling screws with neoprene washers were used to secure the test sheet to the timber supports. The No.14 screws have head and shaft diameters of 14.5 mm and 5.1 mm, respectively and the 2 mm thick neoprene washers have outside and inside diameters of 11 mm and 5 mm, respectively. All the screws were centred at the crests, set

perpendicular to the plane of the sheet and tightened until the neoprene washers were just prevented from rotating to avoid over-tightened or loose screws.

The load per fastener at the central support is an important parameter controlling the pull-through failures (Mahendran, 1994). Therefore two 5 kN load cells were used to measure the loads in two of the central support fasteners. For this purpose the crests of roofing and the central support purlins were predrilled for the insertion of specially made screws. These special screws had the same No.14-10 screw heads, but had a longer shaft (300 mm). The 5 kN load cells were inserted within the longer shaft and tightened with end plates (see Figure 4). In addition to the measurement of individual fastener loads at the central support, the reaction forces at the ends of central and end support purlins were also measured using four 30 kN load cells (see Figure 3a). The latter measurements enabled the determination of the average load per fastener at the central support. The pressure in the air box was monitored by a pressure gauge that had been calibrated with a manometer. It was then used to calculate the nominal load per fastener using a simple formula. Deflections of the steel claddings were measured using five displacement transducers at important locations (see Figure 3).

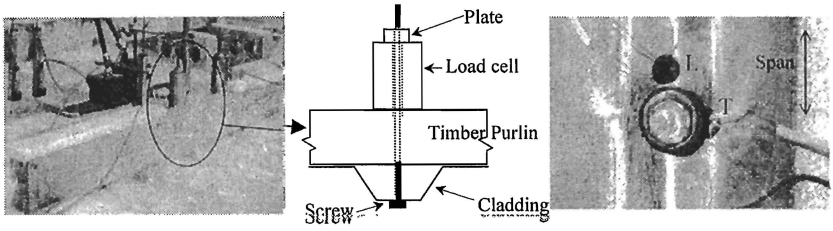

Figure 4. Load Cell and Strain Gauge Arrangement.

In order to accurately determine the strains in the roofing in the vicinity of central support fasteners, eight strain gauges (2 mm gauge length) were used in each test. Since the principal strain directions of the strain field around the central support fastener holes were unknown, three arm 45-degree strain gauge rosettes were placed near the two predrilled fastener holes where the individual load cells were used. The strain gauges were placed in the longitudinal and transverse directions in corresponding positions on both the top and bottom surfaces of the sheeting in order to determine both membrane and flexural strain components (see Figure 4).

In the preliminary tests, two roofing sheets were used as specified in AS 4040.2 (SA, 1992). The use of two sheets gave a specimen width of 1400/1350 mm for Types A and B compared with 820/770 mm for single sheets. The number of central support fasteners was 5 and 8 for single and two-sheet roofing assemblies, respectively.

3. Discussion of Experimental Results.

The results from single and two-sheet roofing assemblies were approximately the same as shown in Figure 5. The single sheet roofing assembly provided a more uniform load distribution among the fasteners, eliminated the additional stiffening problem caused by the lap and simplified the test procedure. Therefore a single sheet roofing assembly was used in most of the tests in this investigation.

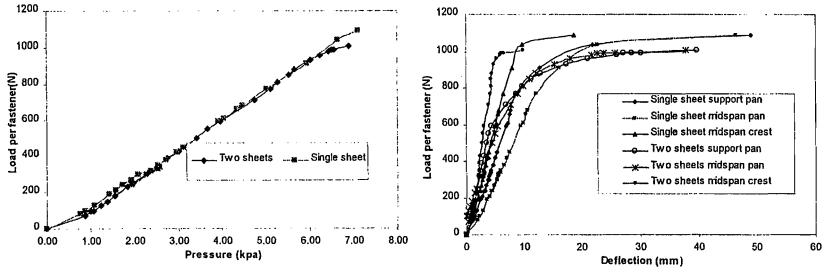

Figure 5. Comparison of Results for Single and Two Sheet Wide Specimens

3.1 Load per fastener

The fastener reaction was the largest at the central support and therefore the local pull-through failures (dimpling or splitting) occurred only at the central support screw fasteners. Tests showed that the failure is governed by the magnitude of the central support load per fastener. The measured individual fastener loads were compared with predictions from simple equations 3 and 4 in Figures 6a and 6b. Equation 3 calculates the load per fastener from the measured uniform pressure based on a two-span beam behaviour whereas Equation 4 was based on a single span beam behaviour.

Load per fastener = 1.25×wind pressure×span×distance between fasteners..(3)

Load per fastener = wind pressure×span×distance between fasteners.....(4)

The average load per fastener was also calculated by dividing the measured central support reaction by n and n-1, where n is the total number of fasteners at the central support (for single sheet roofing assembly, n is 5). This is also plotted in Figures 6a and 6b. Table 1 gives the failure loads.

The load per fastener value from Equation 3 was generally greater than the measured loads. It appeared that the coefficient of 1.25 in the simple formula, which is based on linear theory assuming elastic material and no cross sectional distortion (Mahendran 1994), has to be revised depending on the roofing profile and level of loading. The measured fastener loads are between the average loads per fastener, calculated by dividing the central support reaction by 5 and 4. Therefore the assumption made by the previous researches that the support reaction is distributed uniformly among the fasteners is questionable. Therefore in this paper the measured loads per fastener obtained directly from the individual load cells were used.

Pull-through failure load was calculated by using Equation 1 based on AS 4600 (SA 1996). In these calculations, 75% of the specified minimum strength of G550 steel was used since the steel roof cladding thickness was less than 0.9 mm. The results (Table 1) show that this design formula is incapable of predicting the failure strength of crest-fixed steel cladding systems considered in this investigation. The design formula (Equation 2) recommended by Mahendran and Tang (1999) appears to be

more suitable (Table 1) than the current design formula for the pull-through strength of crest fixed cladding systems, but is also inadequate in some cases.

Table 1. Experimental Failure Loads

Test Cladding and Span (mm)	Fastener reaction (N)	Average load per fastener* (N)		Eq. 3 (N)	Eq.4 (N)	Design Equations (N)	
		4	5			Eq. 1	Eq. 2
Type A-900 mm	1180 1010	1365, 1340	1092, 1170	1418 1657	1135 1357	3248 3248	1186 1186
Type B-900 mm	1060	1225	980	1459	1166	3248	1121
Type A 19 mm washers-900mm	1210	1340	1070	1446	1157	3248	1322
Type A-1000mm	1030 1070	1240 1337	992 1070	1285 1511	1028 1209	3248 3248	1186 1186
Type A-1050 mm	1070	1273	1018	1348	1078	3248	1186
Type A-1100 mm	1100	1258	978	1385	1078	3248	1186
** Type A 20 mm restwidth-425mm	800	1135	908	1184	947	3248	1186
** Type A 26 mm restwidth-425mm	1160	1463	1170	1471	1177	3248	1186
Type B-1100mm	1020	1143	914	1197	957	3248	1121

*4 = Central support reaction /4 5 = Central support reaction /5

** Non-standard profiles which are made in the transverse direction

As seen in Figures 6a and 6b, the load per fastener was approximately linear with upward pressure for loads up to about 600 N. At loads closer to failure, the central support load per fastener suddenly dropped in Type B roofing assembly and then increased further while it was constant and then increased for Type A roofing assembly. This is because the roofing assembly does not behave as a two span beam after local yielding. Instead it behaves as a single span beam. This can be seen in Figures 6a and 6b where the measured fastener loads agree well with Equation 4 predictions after yielding or local failure. Therefore it is reasonably accurate to assume post-failure stage roofing assembly as a single span beam, which implies that in post-local failure deformations, sheeting cross section at the central support sustained only small global bending moments.

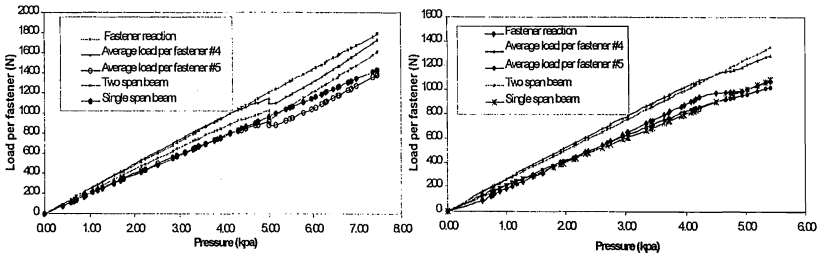

(a) Trapezoidal Type B roofing (b) Trapezoidal Type A roofing

Figure 6. Load per Fastener versus Uplift Pressure Relationship

3.2 Load-deflection Behaviour

Trapezoidal roofing type B

Typical load-deflection curves for this roofing (1100 mm span) are given in Figure 7. They exhibit four stages of behaviour. During the first stage, the behaviour was linear elastic and can be predicted using simple engineering theories. This situation prevails until the fastener reaction reaches around 600 N.

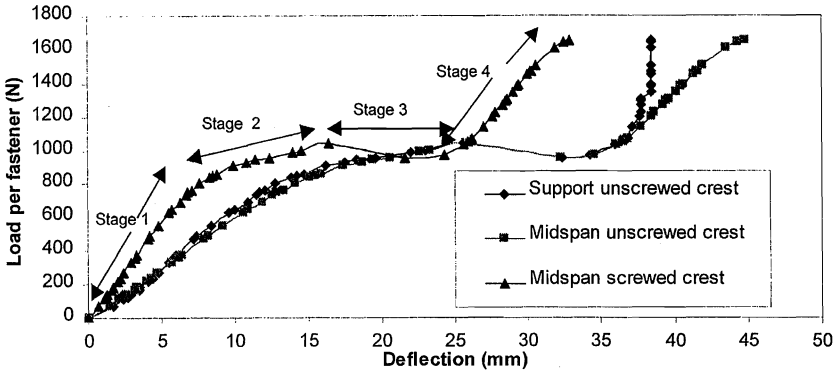

Figure 7. Load-deflection behaviour of trapezoidal type B roofing

With further increase in load, large cross sectional distortions were observed followed by localised deformation and yielding around the fastener holes. These dimples extended further in the longitudinal direction of the sheeting with load increase in the second stage. When the load per fastener reached about 1000 N, large local plastic deformations occurred causing further cross sectional distortion without any load increase. Side plates of the ribs at central fastener buckled with the crest dimpling beyond the edge of the ribs. Although the occurrence of local plastic deformations around the central support fastener could be considered as an initial failure (Mahendran, 1994), the sheet deformed further with the load increasing steadily again during Stage 4. This could be explained by the fact that once side plates flattened, the area around the central fasteners was subject to a membrane behaviour while surrounding sheeting restricted that through large bending strains. This situation continued until the crests and valleys of mid span cross-section began to deform severely that led global plastic mechanisms to form at each midspan when valleys failed by buckling. Soon after this, a pull-through failure occurred in the central support fasteners.

Trapezoidal roofing type A

The load-deflection curves for this roofing of 900 mm and 1100 mm span are presented in Figures 8a and 8b. This has three stages of loading for the small span whilst it behaves similar to type B roofing sheet for the large spans. As for the type B roofing the uplift load caused severe cross sectional distortion since the screwed ribs are separated by a wide pan. For fastener loads up to 600 N the behaviour of roofing was elastic. With increasing loads, the crests slightly dimpled, but not as severe as in

type B roofing. This was followed by a membrane action of the region and plastic dimples became larger. This situation was almost similar for all the spans, but for spans less than 1000 mm, local plastic failure of side plates of ribs can be observed when central support fastener reaction reached around 1200 N and it led to localised pull-through failures. But for span 1100 mm, it showed the strain hardening after plastic failure as for type B roofing. This situation continued until the crests and valleys at midspan began to deform as the type B roofing. But it doesn't have higher capacity like type B roofing since mid span valleys buckled at a smaller load compared with type B roofing. The final failure was similar to type B roofing sheets.

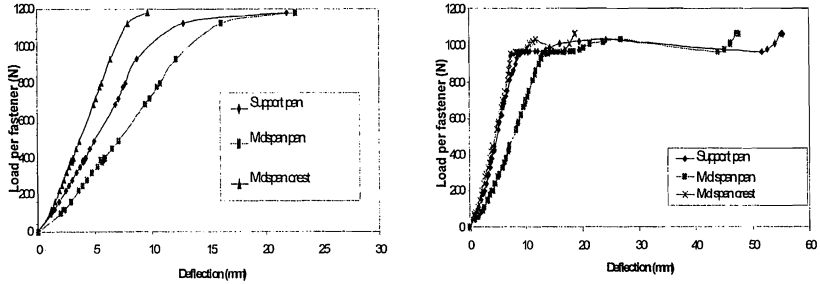

(a) 900 mm span (b) 1100 mm span

Figure 8. Load-deflection behaviour of trapezoidal type A roofing

3.3 Splitting phenomenon

The two-span roofing sheet is subjected to two types of deformations due to global bending of two-span sheets and local bending action around the fastener hole. In the midspan region, the global behaviour dominates and the crests are in tension and valleys in compression. But the roofing sheet around the fastener hole is subject to both global bending effects, and local effects due to fastener reaction. Therefore the crest of roofing sheet around the fastener hole is subjected to a local bending action and a membrane compression force due to global bending.

Tensile testing of G550 steel coupons has shown that it has very little strain hardening and the failure strain is about 2%. This provides some explanation for the premature transverse splitting at the fastener holes. However, the 2% failure strain was obtained for steel in pure tension (membrane only). Its applicability to steel sheet around the fastener hole subject to combined tension and bending actions (membrane and bending) is questionable. Tang (1998) has found that the use of a 2% failure criterion in the finite element analyses did not predict the pull-through failure load of roof sheeting. It should be noted that even G550 steel has a very high strain capacity (more than 30%) for pure bending. This could be demonstrated by subjecting G550 steel coupons to 180° bending without any splitting. Therefore the strain criterion for the sheeting around the fastener holes should be between 2 and 30%.

Experimental strain results were examined to determine an appropriate failure criterion. Figures 9a and 9b present the typical percentage strain variations on the longitudinal and transverse sides of the central support fastener hole. The membrane

strain was obtained by averaging the measured top and bottom surface strains, and the flexural strain obtained by dividing the difference in the surface strains by two.

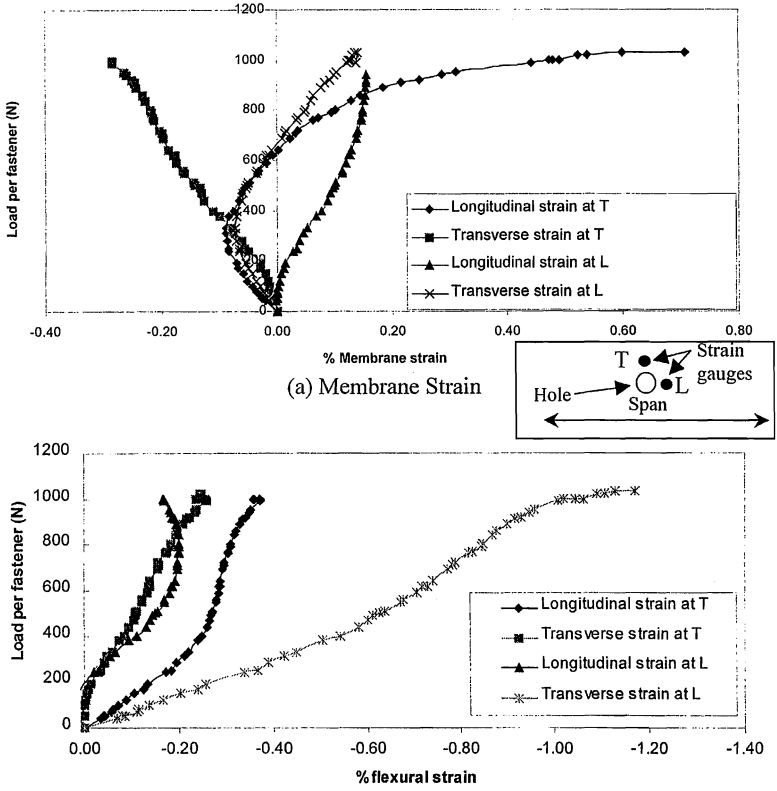

(a) Membrane Strain

(b) Flexural Strain

Figure 9. Variations of Strains – Type A Cladding

The high membrane and flexural strains in the longitudinal direction on the transverse side of the fastener hole indicates why splitting occurs on the transverse side. For smaller uplift pressures, the longitudinal membrane strain on the transverse side was compressive due to the global bending of roofing sheet as a two-span beam. With increasing uplift loads, this situation is modified and the longitudinal membrane strain becomes tension due to the local deformations around the fastener hole. This leads to large local plastic deformations and yielding at the fastener hole. Beyond the stage two loading, the results clearly indicate that redistribution of stresses occurred and strains varied very rapidly. All trapezoidal type B sheets, and some large span type A sheets failed by local dimpling without any splitting. However, other trapezoidal sheets pulled-through at the fastener holes due to transverse splitting. The failure strains including the membrane and flexural components were analysed and tabulated for all tests in Table 2.

Table 2. Comparison of Failure Strains

Experiment	Membrane strain		Flexural strain		Total Strain	Failure
	Strain	% Strain	Strain	% strain		
900 mm span Type A	1.61	67	0.82	33	2.43	Split
	0.84	79	0.22	21	1.07	
900 mm span with 19mm washer Type A	0.45	51	0.44	49	0.89	Didn't split
900 mm span Type B	1.67	48	1.81	52	3.48	Didn't split
1100 mm span Type A	1.77	54	1.5	46	3.27	Didn't split
1100 mm span Type B	1.13	47	1.29	53	2.42	Didn't split
1000 mm span Type A	0.74	71	0.3	29	1.04	Split
	2.31	68	1.1	32	3.4	Split
1050 mm span Type A	0.73	59	0.51	41	1.24	Split
* 425mm span with crest width 20mm Type A	0.69	79	0.17	21	0.82	Split
* 425mm span with crest height 26mm Type A	0.51	80	0.13	20	0.65	Split
Small scale Type A	1.32	68	0.62	32	1.94	Split
Small scale Type A (crest width 20 mm)	1.28	68	0.6	32	1.89	Split
	1.18	68	0.55	32	1.73	Split
Small scale Type A (Crest Height 32 mm)	1.13	65	0.6	35	1.73	Split
Small scale Type A (Pitch 175 mm)	1.54	89	0.2	11	1.74	Split
Small scale Type A (Pitch 210 mm)	1.18	68	0.55	37	1.73	Split
Small scale Type B	1.5	84	0.27	16	1.76	Split

*Non-standard profiles which are made in the transverse direction

From Table 2 results, it can be seen that transverse splitting occurred when the percentage of membrane strain to total strain is more than 60% and the total strain is about 2% and pull-through failure of the connection followed. This is a significant observation than what has previously been assumed in past researches.

The two short span tests on type A roofing (425mm span) showed that the total tensile strains at failure were 0.82 and 0.65%. These values are considerably lower than the 2% value obtained from the other tests. This occurred because these roof sheets were made in the transverse direction. Tensile coupon tests showed that the failure strain of G550 sheets in the transverse direction was 0.8%, which agrees well with the total strain value of 0.82 and 0.65% obtained from the two-span cladding tests. All these results therefore confirmed the strain criteria based on total strain

In a number of two-span cladding tests, the exact failure strains at the moment of splitting could not be recorded because the rate of recording (at 15 sec intervals) of the computer system used was inadequate to handle the rapid variation of strains at failure. Therefore a series of small-scale tests using the method recommended by Mahendran (1994) was conducted as shown in Figure 10. Their results are also included in Table 2. Although the small-scale tests may not produce accurate pull-through failure loads, their results can be used to correlate the strain patterns to splitting. The small-scale test results confirmed that the roofing split when the membrane strain ratio was greater than 65% and the total strain was about 2%. These small-scale experiments also confirmed that splitting initiated on the bottom side of the sheeting where the total tensile strain was the largest.

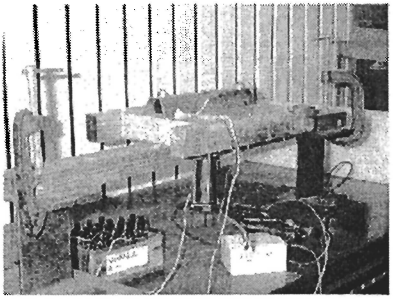

Figure 10. Small Scale Test Set-up

Figure 9b shows that large transverse bending strains exist around the fastener, which explain the severe cross-sectional distortions since the screwed ribs are separated by wide pan of type A roofing or unscrewed crest of type B roofing. Compared with the transverse bending strains, transverse membrane strains were much smaller.

In summary, the series of small scale and large scale steel cladding tests have shown that transverse splitting of high strength steel claddings occurred at the edge of the screw fastener holes (Figure 2a) when

- The membrane strain was 60% of the total strain
- The total tensile strain was equal to the measured failure strain from tensile coupon tests of steel

4. Conclusions and Recommendations

This paper has presented the details of an experimental investigation into the pull-through failure mechanism of crest-fixed thin high tensile steel claddings commonly used in Australia. The results from a large number of full-scale air-box tests and small scale tests on trapezoidal sheeting have been used to develop a strain criterion in terms of the flexural and membrane strain components at the critical central support fastener holes for the transverse splitting observed in the pull-through failures. This strain criterion can be used in numerical modelling of these steel cladding systems. The paper also discusses the nonlinear behaviour of roofing assemblies under wind uplift pressures. It was found that the critical central support fastener loads used in design could not be predicted by conventional simple engineering formulae (Equation 3 and

4) unless appropriate modifications are made to the coefficients in these formulae. The current design formula was unconservative in predicting the pull-through failure loads of crest-fixed steel claddings.

5. References

Beck, V.R. and Stevens, L.K. (1979) Wind Loading Failures of Corrugated Roof Cladding, Civil Eng. Trans., IEAust; 21(1): 45-56.

Mahendran, M. (1990a) Fatigue Behaviour of Corrugated Roofing Under Cyclic Wind Loading, Civil Eng Trans., IEAust; 32(4): 219-226.

Mahendran, M. (1990b) Static Behaviour of Corrugated Roofing Under Simulated Wind Loading, Civil Eng Trans, IEAust; 32(4): 211-218.

Mahendran, M. (1994) Behaviour and Design of Crest Fixed Profiled Steel Roof Claddings Under High Wind Forces, Eng Struct; 16(5): 368-376.

Mahendran, M. and Tang, R.B. (1999) Pull-through Strength of High Tensile Steel Cladding Systems, Australian Journal of Struct. Eng; 2(1): 37-49.

Standards Australia (SA) (1992) AS4040-2 Method of Testing Sheet Roof and Wall Cladding.

Standards Australia (SA) (1996) AS 4600 Cold-formed Steel Structures Code, Sydney.

Tang, R.B. (1998) Local Failures of Steel Cladding Systems Under Wind Uplift, ME Thesis, Queensland University of Technology, Brisbane, Australia.

Xu, Y.L. and Reardon, G.F. (1993) Test of Screw Fastened Profiled Roofing Sheets Subject to Simulated Wind Uplift, Eng. Struct; 15(6): 423-430.